Final Draft
of the original manuscript:

Avdeev, M.V.; Bica, D.; Vekas, L.; Aksenov, V.L.; Feoktystov, A.V.; Marinica, O.; Rosta, L.; Haramus, V.M.; Willumeit, R.

Comparative structure analysis of non-polar organic ferrofluids stabilized by saturated mono-carboxylic acids

In: Journal of Colloid and Interface Science (2009) Elsevier

DOI: 10.1016/j.jcis.2009.03.005

Comparative structure analysis of non-polar organic ferrofluids stabilized by saturated mono-carboxylic acids

M.V.Avdeev[a], L.Vekas[b], V.L.Aksenov[c,a], A.V.Feoktystov[a,d], O.Marinica[e], L.Rosta[f], V.M.Garamus[g], R.Willumeit[g]

[a]Frank Laboratory of Neutron Physics, Joint Institute for Nuclear Research, Dubna, Russia
[b]Center for Fundamental and Advanced Technical Research, Romanian Academy, Timisoara Branch, Romania
[c]Russian Research Center "Kurchatov Institute", Moscow, Russia
[d]Taras Shevchenko Kyiv National University, Physics Department, Kyiv, Ukraine
[e]National Center for Engineering of Systems with Complex Fluids, University Politehnica Timisoara, Timisoara, Romania
[f]Research Institute for Solid State Physics and Optics, Budapest, Hungary
[g]GKSS Research Centre, Geesthacht, Germany

Abstract

The structure of ferrofluids (magnetite in decahydronaphtalene) stabilized with saturated mono-carboxylic acids of different chain lengths (lauric, myristic, palmitic and stearic acids) is studied by means of magnetization analysis and small-angle neutron scattering. It is shown that in case of saturated acid surfactants, magnetite nanoparticles are dispersed in the carrier approximately with the same size distribution whose mean value and width are significantly less as compared to the classical stabilization with non-saturated oleic acid. The found thickness of the surfactant shell around magnetite is analyzed with respect to stabilizing properties of mono-carboxylic acids.

Keywords: magnetic fluids; magnetic nanoparticles; magnetite; mono-carboxylic acids; fatty acids; stabilization.

1. Introduction

The nature of surfactant used for coating particles in magnetic fluids (MFs), fine liquid dispersions of magnetic materials, is an important factor, which determines colloidal stability of these systems. In this work we report our results on structural studies of new MFs based on non-polar organic carrier (magnetite dispersed in decahydronaphtalene, DHN). It is well known [1] that one of the best molecules for stabilizing magnetite nanoparticles in such type of carriers is oleic acid (OA), a non-saturated mono-carboxylic (fatty) acid, which has a C_{18}–tail with a double bond kink in the middle. Its polar head is well adsorbed on the surface of magnetic particles (chemisorption), while hydrophobic tails dissolve in the carrier. Despite wide use of this surfactant in stabilization procedures of magnetic fluids, still there is no full understanding what factors responsible for the resulting stabilization distinguish oleic acid from its straight-chain saturated analogue, stearic acid, which always is considered as a poor stabilizer [1, 2].

Here, we apply the stabilization procedure well-proven for OA, to a series of saturated and straight carboxylic acids of various chain lengths, namely lauric (LA), myristic (MA), palmitic (PA) and stearic (SA) acids with C_{12}, C_{14}, C_{16}, C_{18}- tails, respectively. In principle, the possibility for using LA and MA in this procedure was shown previously [3, 4]. The significant difference in the viscosity and magnetoviscous effect in MA- and OA-stabilized fluids were also reported [4, 5]. Despite the relatively low dispersing efficiency of probed saturated acids as compared to OA we succeeded in the synthesis of stable and rather concentrated samples (volume fraction of magnetic nanoparticles, φ_m, above 10 %). The comparison of the structure of these fluids with the classical fluid stabilized by OA is made by means of the magnetization analysis and small-angle neutron scattering, which deal with bulk samples. The main aspects of the comparison are the resulting particle size distribution of magnetite and the effective thickness of the surfactant shell.

2. Materials and methods

All studied fluids were prepared at the Center for Fundamental and Advanced Technical Research, Romanian Academy, Timisoara branch, Romania, by the same procedure [6, 3] standard for OA stabilization. Magnetite nanoparticles, Fe_3O_4, were obtained by the co-precipitation in aqueous solution of Fe^{2+} and Fe^{3+} ions (salts $FeSO_4.7H_2O$; $FeCl_3.4H_2O$) in the presence of NH_4OH sol. 25%, at the temperature 80-82^{o}C. This value of the temperature and the significant excess amount of NH_4OH ensured the formation of magnetite over other iron oxides [6]. A surfactant from the above mentioned series was added in a significant excess (30 vol. %) to the system right after the co-precipitation starts, following the chemisorption of acids on the magnetite surface. Then, several steps including washing with magnetic decantation, flocculation, re-dispersion in light hydrocarbon and filtration were performed to remove residues of salts, free surfactant in solution and large aggregates of non-dispersed magnetic particles, respectively. Finally, magnetic particles coated with a single surfactant layer were extracted by flocculation with acetone and, then, re-dispersed into the required carrier, DHN (Merck, chemically pure). The particle concentration in the MF after the described procedure strongly depends on the acid used. Despite the fact that exact quantitative analysis of the dispersing efficiency is quite a difficult topic for colloidal solutions, qualitatively we conclude that as compared to OA such efficiency is just several times less for MA, and more than 10 times less for other saturated acids (LA, PA, SA). Again, qualitatively, SA is the worst stabilizant among the considered saturated acids. Repeating several times the above procedure in the case of saturated acids (depending on their dispersing efficiency), we succeeded to concentrate the samples up to φ_m within 6 - 10 %. It is important to note that the final flocculation-redispersion cycle was additionally performed until the free surfactants were completely removed from the fluids. The approximate ratio between volume fractions of magnetite and covering surfactants was determined from density measurements and constituted 1:1 for OA sample and between 1:2 and 1:3 for samples with saturated acids. All of the obtained fluids showed excellent stability and

retained their properties in respect to the effect of external magnetic field and time at least a year later.

The magnetization analysis was performed on the MFs diluted down to $\varphi_m \approx 1.5$ %. The full magnetization curves up the maximal applied field of 800 kA/m were obtained using the vibrating sample magnetometer VSM 880 (DMS/ADE Technologies-USA) of the NCESCF-UP Timisoara. For SANS experiments two kinds of samples were prepared by diluting the initial MFs down to $\varphi_m < 1$ % with usual and deuterated DHN (d-DHN, 99 %, Deutero Gmbh), respectively. The d-DHN content in all samples of the second kind was 90 %.

SANS investigations of the above samples (non-polarized mode, no magnetic field at the sample) were performed on the small-angle instruments SANS-1 at the GKSS Research Centre [7] and "Yellow Submarine" at the Budapest Neutron Center. The differential cross-section per sample volume (scattering intensity) isotropic over the radial angle φ on the detector plane was obtained as a function of the momentum transfer module, $q = (4\pi/\lambda)\sin(\theta/2)$, where λ is the incident neutron wavelength and θ is the scattering angle. On SANS-1 measurements were made at a neutron wavelength of 0.81 nm (monochromatization $\Delta\lambda/\lambda = 10\%$) and a series of sample-detector distances (SDD) within the interval of 0.7 ÷ 9.7 m (detector size 55 cm) to cover a q-range of 0.06 ÷ 2 nm^{-1}. A standard procedure was applied to calibrate the cross-section on a water sample of 1 mm thickness [8], together with the corrections on the background, container scattering and incoherent background (subtraction of the scattering from corresponding buffer). At large sample-detector distances (> 4.5 m) the calibrating patterns were obtained by the recalculation of the curves for H_2O at the SDD of 1.8 m with corresponding distance coefficients. On the "Yellow Submarine" facility the fixed wavelength of 0.45 nm (monochromatization $\Delta\lambda/\lambda = 13$ %) and sample-detector distances of 2 and 5.5 m (detector size 64 cm) were used to cover the q-interval of 0.01-4 nm^{-1}. The same H_2O calibration procedure was applied. At both instruments samples and buffers were put into 1 mm thick quartz cells (Hellma) and were kept at room temperature (25 °C) during the expositions.

3. Results and discussion

The main structural difference revealed for the fluids with saturated acids as compared to the OA case concerns the size distribution function of the stabilized magnetite nanoparticles.

First, the size distributions were inferred from the magnetization curves (Fig.1). They were treated assuming the log-normal distribution of the magnetite radius R:

$$D_N(R)=(1/(2\pi)^{1/2}SR)\exp[-\ln^2(R/R_0)/(2S^2)], \quad (1)$$

with parameters R_0, S. The polydisperse Langevin approximation [9] was used:

$$M(H)/M_s = \int D_N(R)L(\mu_0\mu V(R)H/k_BT)dR, \quad (2a)$$

$$L(x) = \mathrm{cth}\, x - 1/x, \quad (2b)$$

where M_s is the saturation magnetization; $\mu = 4.46\times10^{-5}$ A J m^{-4} is the specific magnetic moment of magnetite; $V(R)$ is the volume of spherical particles of radius R; k_B is the Boltzmann constant; T is the temperature; $L(x)$ is the Langevin function. Because of the comparatively low volume fraction of magnetite, both the concentration effect and the magnetic interaction were not taken into account. The resulting values of the varied parameters R_0, S are given in Table 1. The numerical data on "magnetic" sizes evidence a significant difference between the OA stabilized sample in comparison with those stabilized with saturated carboxylic acids.

The SANS curves also clearly show a great difference in the $D_N(R)$ functions. This fact is the most transparent when scattering is registered for usual (non-deuterated) DHN (Fig.2). Since the scattering length densities (SLDs) of the surfactant, ρ_1, and the carrier, ρ_s, are very close (ρ_1, ~ ρ_s ~ 0), the scattering from the surfactant layer is matched. Also, the nuclear scattering dominates strongly over the magnetic part, which is a result of the large contrast between magnetite and carrier [10]. So, the curves in Fig.2 correspond to the nuclear scattering from

magnetite and can be treated in the frame of the model of homogeneous polydisperse spheres [10] with the particle size distribution function of type (1):

$$I(q) = \frac{I(0)}{< V^2(R) >_R} \int V^2(R) D_N(R) \Phi^2(qR) dR + B\,, \qquad (3a)$$

$$I(0) = n(\rho - \rho_s)^2 < V^2(R) >_R \qquad (3b)$$

$$\Phi(x) = 3\frac{\sin(x) - x\cos(x)}{x^3}\,. \qquad (3c)$$

Here, $I(0)$ and B are additional varied parameters corresponding to the forward scattering intensity and background, respectively. Parameter $I(0)$ is expressed through the particle number density, n; squared difference between scattering length densities (contrast) of the particle, ρ_0, and carrier, ρ_s; and mean squared particle volume. The $\Phi(qR)$ function is the form-factor of a spherical particle with radius R. One can see good fits of this model to experimental curves in Fig.2, whose results concerning characteristic sizes are gathered also in Table 1.

The difference in the data of magnetization analysis and SANS can be seen for $D_N(R)$. It is most significant for the case of the OA stabilization. In [3] it was claimed that if this difference is due to the non-magnetic layer at the surface of magnetite particles, the thickness of such layer should depend on the particle size. However, there is no clear evidence for such effect. In this respect, another reason may be assumed related to a small magnetic interaction effect, which can concern both the magnetization analysis and SANS. In the first case, it influences the used Langevin approximation. The larger the particles dispersed in the liquid (OA sample), the stronger the interaction; hence, a larger deviation in the parameters of the Langevin approximation can take place. In SANS the attraction between particles results in appearance of the scattering structure-factor; this increases the apparent size of the particles and makes it different from what is seen in magnetization analysis. This is confirmed by recent results of the SANS contrast variation on ionic water-based fluids, where the difference in the effective nuclear and magnetic radii was found to be about 3 nm [11]. The limiting case of such interaction is the formation of some agglomerates. If the effect of the agglomerates is small, it results just in the effective increase of the apparent atomic size observed in the nuclear scattering contribution. At the same time, despite the interaction the magnetic moments cannot be correlated over the whole size of agglomerate. Hence, in the presence of agglomerates the effective magnetic size, which is determined in the magnetization analysis, is always smaller than the averaged atomic particle size.

The thickness of the surfactant layer around magnetite nanoparticles can be deduced from SANS data for 90% d-DHN solutions, as in Fig.3. In this case, due to a significant contrast (ρ_s = 6.545×10^{10} cm^{-2}) the scattering from the layer contributes much in the curves making their behavior quite different from the previous case with usual DHN. The modulation of the scattering with the chain length of the saturated acids is clearly seen in Fig.3*a*. Since the particle size distribution does not change much with the surfactant, and the scattering length densities of the saturated acids are very close, the surfactant chain length is the only factor determining the difference in the curves for saturated acids. The given data differ from those in Fig.2, where no modulation on the surfactant length takes place. Again, the curve for the fluid with the OA stabilization in Fig.3*a* shows qualitatively different behavior as compared to saturated acids, which confirms the conclusion about the difference in the $D_N(R)$ function for the two cases. In Fig.3*b* all curves are fitted to the core-shell model for particles with polydisperse cores [12]:

$$I(q) = \frac{I(0)}{< [V(R) + \eta V(R+h)]^2 >_R} \int_{R_{\min}}^{R_{\max}} D_N(R) [V(R)\Phi(qR) + \eta V(R+h)\Phi(q(R+h))]^2 dR + B \qquad (4a)$$

$$I(0) = n < [V(R) + \eta V(R+h)]^2 >_R \qquad (4b)$$

Here, like in (3) R is referred to the radius of magnetite; h denotes the effective thickness of the surfactant layer; and the dimensionless parameter η=-(ρ_1 - ρ_s)/ (ρ_1-ρ_0) was varied around the calculated value of –0.95. Also, the parameters of the $D_N(R)$ function were free only over 5 % vicinities around the values taken from the data in Fig.2. In (4) the magnetic scattering contribution is neglected. As it was shown previously [13, 12, 14], it is difficult to model this contribution because of the complex magnetic correlations. Nevertheless, its effect is small for q > 0.1 nm^{-1} [13, 12, 14]. At smaller q-values it results in systematic deviation of the experimental data from the model curves (see Fig.3*b*). The resulting h-values are presented in Table 1. They confirm the conclusion that the thickness of the surfactant layer correlates with the surfactant length, L, whose value calculated according to Tanford's formula [15] is given in Table 1 for comparison. Taking into account the fact that saturated fatty acids of various chain lengths stabilize magnetite nanoparticles with approximately the same $D_N(R)$, one can conclude that this $D_N(R)$ is not determined by the acid chain length, but rather by the organization of acid molecules on the magnetite particle's surface. Our data show that a stabilizing layer of a saturated acid manifests worse elastic properties than the layer of OA.

The other reason, which can affect the stabilized particle size distribution, as well as the dispersing efficiency of the acids, is connected with chemical factors during the preparation procedure. Thus, the possible micelle formation in intermediate water solutions can decrease the number of free surfactant molecules required for full coating of magnetite surface. The critical micelle concentration is inversely proportional to the molecule length [16], which correlates with the worst dispersing efficiency of the longest chain surfactant SA. Also, concentrated solutions of strongly anisotropic molecules are characterized by a transfer to the nematic phase, which also affects the number density of free surfactant in solution. The addition of the surfactants during the synthesis of the studied MFs is performed using concentrated solutions of the acids in light hydrocarbon, where the nematic phase can form. The careful consideration of these two points is the subject of our further research.

It is important to mention that we can exclude the possible influence of free surfactants in the final MFs on the discussed properties. First, as it was noted a special procedure was applied to remove free surfactants as much as possible. Second, our experiments with pure surfactant solutions [17], as well with deliberate surfactant excess in the studied type of MFs [18] show that specific effects can be expected at the surfactant volume fraction above 10 %, which is definitely not the case in the present work.

It should be also pointed out that the procedure applied for stabilization is quite reproducible. Two independent preparations of MF samples were made, which repeat the found effects.

4. Conclusion

To summarize, the stabilization procedure for non-polar organic magnetic fluids probed first with short chain length carboxylic acids (LA and MA) was successfully repeated and also widened for longer chain length acids from this series (PA, SA). The significant difference between this series of saturated chain length surfactants and oleic acid (OA) in stabilizing MF samples was evidenced by magnetogranulometric and SANS analyses. Despite the different thickness, the shells of the saturated acids around magnetite nanoparticles in the studied MFs exhibit similar stabilizing properties as it concerns the size distribution functions of the dispersed nanoparticles. Along with it, these acids are characterized by different dispersing efficiency. To explain the found effect, in addition to the energetic conditions of the MFs stabilization (elastic properties of the surfactant layer), chemical factors during preparation (presumably, formation of various aggregates) should be carefully considered.

The work was done in the frame of the project Helmholtz-RFBR (HRJRG-016).

The MF samples investigated were synthesized by Dr. Doina Bica† (1952-2008) in the framework of the research program of the Lab. Magnetic Fluids-CFATR; this work is dedicated to her memory. The researches have also been supported by the European Commission under the 6th Framework Program through the Key Action: Strengthening the European Research Area, Research Infrastructures. Contract nr: RII3-CT-2003-505925, GKSS, Germany; Agreement between JINR and Hungarian Academy of Sciences, as well as by the CEEX research program of the Romanian Ministry of Education and Research, contract NanoMagneFluidSeal nr.83/2006.

References

[1] R.E. Rosensweig, Ferrohydrodynamics, Cambridge University Press, Cambridge, 1985.
[2] R. Tadmor, R.E. Rosensweig, J. Frey, J. Klein, Langmuir 16 (2000) 9117.
[3] M.V. Avdeev, D. Bica, L. Vékás, et al., J. Mag. Mag. Mater. 311 (2007) 6.
[4] L. Vékás, D. Bica, O. Marinica, Rom. Rep. Phys. 58 (2006) 257.
[5] L. Vekas, D. Bica, M.V. Avdeev, China Particuology 5 (2007) 43.
[6] D. Bica, Rom. Rep. Phys. 47 (1995) 265.
[7] H.B. Stuhrmann, N. Burkhardt, G. Dietrich, et al., Nucl. Instrum. Methods A 356 (1995) 133.
[8] B. Jacrot, Rep. Prog. Phys. 39 (1976) 911.
[9] M. Rasa, Eur. Phys. J. 2 (2000) 265.
[10] M.V. Avdeev, V.L. Aksenov, M. Balasoiu, et al., J. Colloid Interface Sci. 295 (2006) 100.
[11] R. Perzinsky, E. Dubois, V. Garamus, et al., In GeNF Annual Report 2005, GKSS, 2006.
[12] M.V. Avdeev, M. Balasoiu, V.L. Aksenov, et al., J. Mag. Mag. Mater. 270 (2004) 371.
[13] M.V. Avdeev, M. Balasoiu, Gy. Torok, et al., J. Mag. Mag. Mater. 252 (2002) 86.
[14] M.V. Avdeev, Physics Uspekhi 50 (2007) 1083.
[15] C. Tanford, J. Phys. Chem. 76 (1972) 3020.
[16] B. Jounsson, B. Lindman, K. Holmberg, B. Kronberg, Surfactants and polymers in aqueous solution, John Wiley & Sons, Chichester, 1998.
[17] V.I. Petrenko, M.V. Avdeev, L. Almásy, et al., J. Colloids Surf. A, accepted (2008).
[18] V.I. Petrenko, M.V. Avdeev, V.L. Aksenov, et al., Adv. Mater. Res., accepted (2008).

Table 1

Sample	R_0, nm		S		h, nm (scattering)	L, nm
	magnetization	scattering	magnetization	scattering		
OA	2.70	3.40	0.39	0.38	1.40	2.3
SA	2.50	2.55	0.22	0.28	1.85	2.3
PA	2.40	2.48	0.22	0.28	1.55	2.1
MA	2.40	2.65	0.22	0.28	1.35	1.8
LA	2.30	2.51	0.22	0.28	1.25	1.6

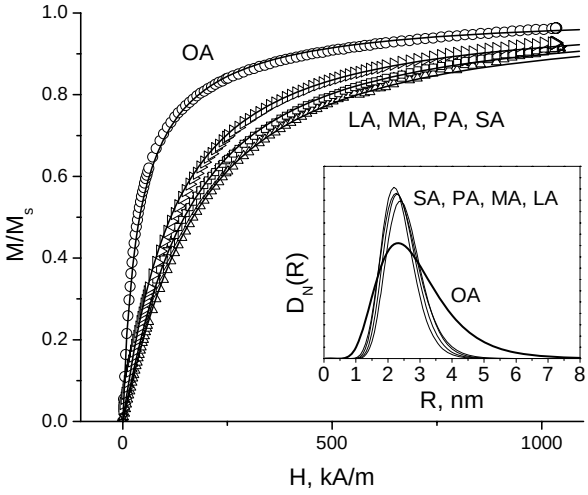

Fig.1. Magnetization curves (points) for magnetic fluids stabilized by various mono-carboxylic acids in DHN, φ_m = 1.5 %. Lines are the results of the polydisperse Langevin approximation. Inset shows the corresponding particle size distributions of magnetite (magnetic size).

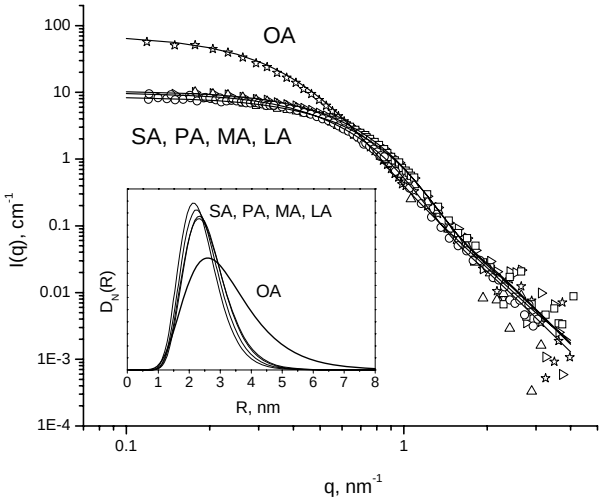

Fig. 2. SANS curves (points) for MFs in DHN normalized to φ_m = 1.5 %. Lines are the results of approximation by the model of poly-disperse independent spheres. Inset shows the corresponding particle size distributions of magnetite (atomic size).

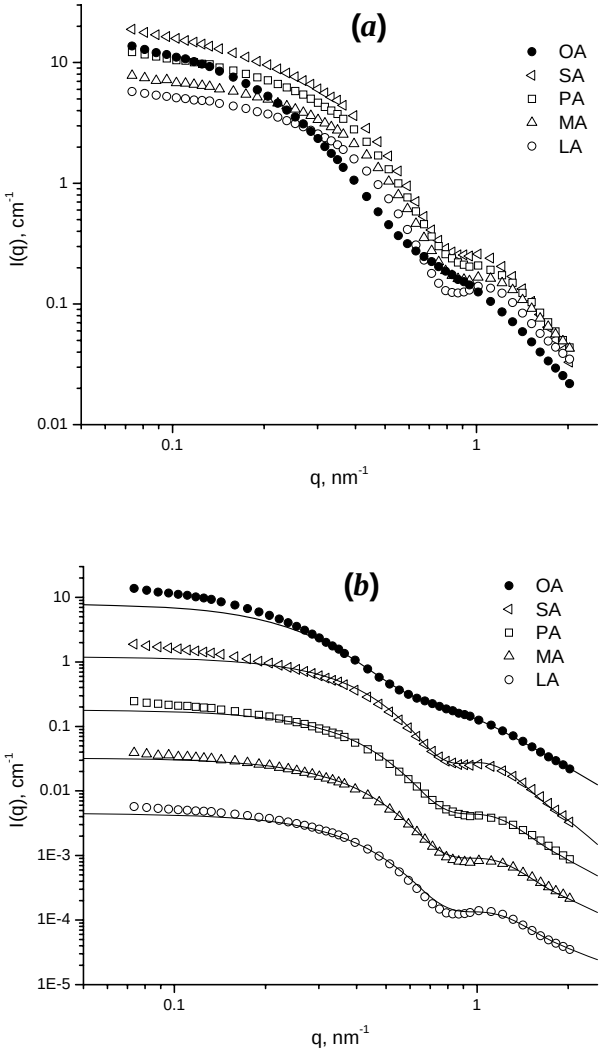

Fig.3. SANS curves for MFs in 90 % d-DHN. (*a*) curves are normalized to φ_m = 0.6 %. (*b*) approximation by the model of independent core-shell particles with polydisperse core; for convenient view the curves are additionally divided by factors of 10 (SA), 50 (PA), 200 (MA), 1000 (LA).